

# Test of the universality of free fall with atoms in different spin Orientations

Xiao-Chun Duan, Min-Kang Zhou, Xiao-Bing Deng, Hui-Bin

Yao, Cheng-Gang Shao, Jun Luo, and Zhong-Kun Hu\*

*MOE Key Laboratory of Fundamental Physical Quantities Measurements,*

*School of Physics, Huazhong University of Science and Technology,*

*Wuhan 430074, People's Republic of China*

(Dated: August 18, 2019)

## Abstract

We report a test of the universality of free fall (UFF) related to spin-gravity coupling effects by comparing the gravity acceleration of the  $^{87}\text{Rb}$  atoms in  $m_F = +1$  versus that in  $m_F = -1$ , where the corresponding spin orientations are opposite. A Mach-Zehnder-type atom interferometer is exploited to sequentially measure the free fall acceleration of the atoms in these two sublevels, and the resultant Eötvös ratio determined by this work is  $\eta_S = (-0.2 \pm 1.5) \times 10^{-5}$ . The interferometer using atoms in  $m_F = +1$  or  $m_F = -1$  is highly sensitive to magnetic field inhomogeneity, which limits the current experimental precision of our UFF test. The work here provides a stepping stone for future higher precision UFF test related to different spin orientations on atomic basis.

PACS numbers: 37.25.+k, 03.75.Dg, 04.80.Cc

The universality of free fall (UFF) is one of the fundamental hypotheses in the foundation of Einstein’s general relativity (GR) [1], which states that all test bodies fall with the same acceleration in the gravitational field regardless of their structure and composition. Traditional verifications of the UFF are performed with macroscopic bodies that weight differently or comprise of different material by torsion balance technique [2–4], free-fall method [5–7] or laser ranging mission [8, 9], achieved a level of  $10^{-13}$  [3, 4, 9]. There are also lots of work investigating possible violation of UFF that may be induced by spin-related forces (see, for example, [10–15]), and UFF tests of this kind have been performed with polarized or rotating macroscopic bodies [16–24]. Here we report a spin-orientation related UFF test with quantum objects by atom interferometry.

UFF tests with quantum objects have earlier been performed with a neutron interferometer [25], and in recent years, were carried out by comparing the free fall acceleration between different atoms or between atoms and macroscopic masses [26–31]. The motivation of using quantum objects is not only for potentially higher precision or associated well defined properties, but also for more possibilities to break Einstein equivalence principle on quantum basis [32]. For example, the variation of the free fall acceleration with atoms in different hyperfine levels has also been tested in Ref. [27] at a level of  $10^{-7}$ . Recently, Tarallo et al. [33] performed an UFF test using the bosonic  $^{88}\text{Sr}$  isotope ( $I = 0$ ) and the fermionic  $^{87}\text{Sr}$  isotope ( $I = 9/2$ ) at a level of  $10^{-7}$  by Bloch oscillation. In their experiment, the  $^{87}\text{Sr}$  atoms were in a mixture of different magnetic sublevels, resulting in effective sublevel of  $\langle m_F \rangle = 0$ . They also gave an upper limit on the spin-gravity coupling by analyzing the broadening caused by possible different free fall accelerations between different magnetic sublevels. However, we note that possible anomalous spin-spin couplings (see, for example, [20, 34, 35]) or dipole-dipole interaction (see, for example, [36]) between the  $^{87}\text{Sr}$  atoms with different magnetic sublevels may disturb, or even cover the spin-gravity coupling effects in their experiment. Since most models describing spin-gravity coupling imply a dependence on the orientation of the spin, we perform a new UFF test with  $^{87}\text{Rb}$  atoms sequentially prepared in two opposite spin orientations (Fig. 1), namely  $m_F = +1$  versus  $m_F = -1$ . The corresponding free fall accelerations are compared by atom interferometry [37–41], which determines the spin-orientation related Eötvös ratio [42] as

$$\eta_S \equiv 2 \frac{g_+ - g_-}{g_+ + g_-}. \quad (1)$$

In Eq.(1), the gravity acceleration of atoms in  $m_F = +1$  ( $m_F = -1$ ) is denoted as  $g_+$  ( $g_-$ ) to account for possible difference. This provides a direct way to test spin-orientation related UFF on quantum

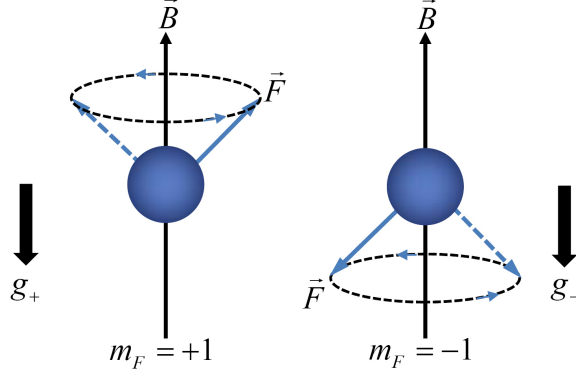


FIG. 1: (color online) Schematic of the spin orientations for  $^{87}\text{Rb}$  atoms in magnetic sublevels  $m_F = +1$  versus  $m_F = -1$  of the  $5^2S_{1/2}$  hyperfine levels. The bias magnetic field  $\vec{B}$  defines the external direction to which the atoms spin is referenced. And the total angular momentum of each atom (denoted by the  $\vec{F}$ ) precesses around  $\vec{B}$ .

basis.

Compared with UFF tests using polarized or rotating macroscopic masses, it is much simpler to prepare cold atomic ensemble with pure polarization using stimulated Raman transition [43]. However, with atoms in sublevels  $m_F = +1$  or  $m_F = -1$ , the Zeeman effect is considerable, which makes the interferometer highly sensitive to the magnetic field inhomogeneity. What's worse is that the phase shift induced by the inhomogeneity is opposite for atoms in the two sublevels, which thus can't be directly canceled in the final comparison of measured free fall accelerations. For the interferometer with atoms in  $m_F$ , the phase shift induced by the gravitational acceleration and the magnetic field gradient is expressed as

$$\varphi_{m_F}^{\pm} = \mp k_{\text{eff}} g_{m_F} T_{\text{eff}}^2 + 2\alpha_{Z,I} m_F \gamma_B (V_{\pi} \mp V_r/2) T^2, \quad (2)$$

where the superscript  $\pm$  denotes the corresponding direction of  $\mathbf{k}_{\text{eff}}$  in the interfering process, with  $+k_{\text{eff}}$  ( $-k_{\text{eff}}$ ) indicating the same (opposite) directions between  $\mathbf{k}_{\text{eff}}$  and local gravitational acceleration. And  $T$  is the separation time between Raman laser pulses, while  $T_{\text{eff}} \equiv T \sqrt{1 + 2\tau/T + 4\tau/\pi T + 8\tau^2/\pi T^2}$  is the effective separation time accounting for the effect of finite Raman pulses duration ( $\tau$  is the duration for the  $\pi/2$  Raman pulse) [37]. In Eq.(2), the second term corresponds to that induced by the magnetic field (only the first order of the inhomogeneity is considered), where  $\gamma_B$  is the magnetic field gradient,  $\alpha_{Z,I}$  is the strength of first-order Zeeman shift for  $^{87}\text{Rb}$  atoms in  $5^2S_{1/2}$  state,  $V_r$  is the recoil velocity, and  $V_{\pi}$  is the average vertical velocity of the atoms in  $F = 1$  at the moment of the interfering  $\pi$  pulse (in this work, the atoms are initially

prepared in  $F = 1$  before the interfering).

In order to alleviate the influence of the magnetic field inhomogeneity, according to Eq. (2), three steps are taken in this work. Firstly, the magnetic field throughout the interfering space is mapped [44, 45], and a region where the field is relative homogeneous is selected for the interfering to take place, namely making  $\gamma_B$  as small as possible. The selected region is at about 736 mm height above the magnetic-optical trap (MOT) center. And there the magnetic field varies less than 0.1 mG over several-millimeters vertical distance, while the magnitude of the bias magnetic field is about 115 mG. Secondly, the direction of the effective Raman laser wave number  $\mathbf{k}_{\text{eff}}$  can be reversed to make a differential measurement for each  $m_F$  [37]. A majority of the influence (the part associated with  $V_\pi$  in Eq. (2)) induced by the magnetic gradient will be canceled using this differential measurement, since the influence is almost independent off  $\mathbf{k}_{\text{eff}}$  (we note that  $V_\pi$  is typically much larger than  $V_r$ ). However, with the Raman lasers configured in  $+k_{\text{eff}}$  versus  $-k_{\text{eff}}$ , the directions of the recoil velocities are opposite. This induces a tiny difference between the atoms' trajectories. And consequently causes a residual influence in the differential measurement result, which is the part associated with  $V_r$  in Eq. (2). The third step is to correct this residuum using the  $\gamma_B$  obtained from the common mode result for the two interfering configurations of  $\mathbf{k}_{\text{eff}}$ . According to Eq.(2), for each  $m_F$ , the differential mode measurement result ( $\Delta\varphi_{m_F}^d \equiv (\Delta\varphi_{m_F}^+ - \Delta\varphi_{m_F}^-)/2$ ) and the common mode measurement result ( $\Delta\varphi_{m_F}^c \equiv (\Delta\varphi_{m_F}^+ + \Delta\varphi_{m_F}^-)/2$ ) are respectively

$$\begin{cases} \Delta\varphi_{m_F}^d = -k_{\text{eff}}g_{m_F}T_{\text{eff}}^2 - \alpha_{Z,I}m_F\gamma_B V_r T^2 \\ \Delta\varphi_{m_F}^c = 2\alpha_{Z,I}m_F\gamma_B V_\pi T^2 \end{cases} . \quad (3)$$

According to Eq.(3), the magnetic field gradient  $\gamma_B$  can be directly estimated from  $\Delta\varphi_{m_F}^c$ , as long as  $V_\pi$  is known.

In order to maximally suppress the magnetic-field-gradient influence in the differential measurement for each  $m_F$ , it is required that both  $\gamma_B$  and  $V_\pi$  are the same between the  $+k_{\text{eff}}$  and  $-k_{\text{eff}}$  interfering configurations. The two requirements can be simultaneously satisfied by preparing the atomic ensembles in the same average velocity, namely  $V_s^+ = V_s^-$  ( $V_s$  denotes the average velocity of the atomic ensemble after the state preparation, and the superscript  $\pm$  denotes the  $\mathbf{k}_{\text{eff}}$  configuration). In this case, the atomic ensembles are in the same region when the interfering is taking place, and thus  $\gamma_B$  is the same, while  $V_\pi$  is obviously the same since it is directly determined by  $V_s$ . Though techniques are mature for preparing the atoms state by velocity-sensitive Raman transition (VSRT) [43], it is in fact not simple to ensure the equality between  $V_s^+$  and  $V_s^-$ . Using conventional state preparation method (see, for example, [46]), the equality will strongly depend

on the pre-determined Zeeman shift and AC-Stark shift. And the corresponding variations will cause opposite changes for  $V_s^+$  and  $V_s^-$ . Here we explore an easy but reliable method to guarantee this equality. For the two interfering configurations, we implement the state preparations using the Raman lasers both configured in  $+k_{\text{eff}}$  with the same effective frequency  $\omega_{\text{eff}}$  ( $\omega_{\text{eff}} \equiv \omega_1 - \omega_2$ , namely the frequency difference of the two laser beams in Raman lasers.). In this case, for each  $m_F$ , the state preparations are completely the same for the two interfering configurations, and thus the average velocities of the selected atoms  $V_s$  are naturally the same. Compared with conventional operation of the interferometer, in addition to usual Raman lasers frequency chirp, this method needs an extra shift of  $\omega_{\text{eff}}$  after the state preparation. This shift will switch the Raman lasers configuration from  $+k_{\text{eff}}$  to  $-k_{\text{eff}}$  for the interfering process where the Raman lasers need to be configured in  $-k_{\text{eff}}$ . This can be realized by using two arbitrary function generators (AFG) to mix with a microwave signal source in the Raman lasers' optical phase locking loop (OPLL), with one AFG to implement the  $\omega_{\text{eff}}$  shift and the other to implement the chirp.

The experiment is performed in an atom gravimeter that has been previously reported in detail in Ref. [40]. It takes 727 ms to load about  $10^8$  cold  $^{87}\text{Rb}$  atoms from a dispenser using a typical MOT. Then the atoms are launched upward and further cooled to about 7  $\mu\text{K}$  with a moving molasses procedure in the atomic fountain. The apex of the fountain is at 750 mm height above the MOT, close to the aimed interfering region at about 736 mm, which is helpful to limit the atoms' flying distance during the interfering process. After a flight time of 324 ms from the launch, a Raman  $\pi$  pulse with a duration of 26  $\mu\text{s}$  is switched on to implement the state preparation. With the Raman lasers configured in  $+k_{\text{eff}}$ , the detune (defined here as the difference between  $\omega_{\text{eff}}$  and the hyperfine splitting of the two ground levels ( $5^2S_{1/2}$ ) of the  $^{87}\text{Rb}$  atom) that selects the maximum  $m_F = +1$  atoms is found to be  $-1546$  kHz, and that for  $m_F = -1$  is  $-1866$  kHz. After the unwanted atoms are removed by a blow-away beam, the atomic cloud arrives at 736mm height and undergoes the  $\pi/2 - \pi - \pi/2$  Raman pulses with a pulse separation time of  $T = 2$  ms. With larger  $T$ , the interferometry fringe would become invisible due to different magnetic field inhomogeneity experienced by respective atom in the ensemble. This is the reason why the effect of the finite Raman pulses durations must be considered in Eq. (2). The transition probability of the atoms after the interfering is obtained through a normalized fluorescence detection when the clouds falls back into the detection chamber. The entire process of a single shot measurement as described above takes 1.5 s. Before the formal data acquisition,  $V_\pi$  should be measured to deduce  $\gamma_B$  from  $\Delta\varphi_{m_F}^c$ . This velocity can be obtained from the spectroscopy of the VSRT [43]

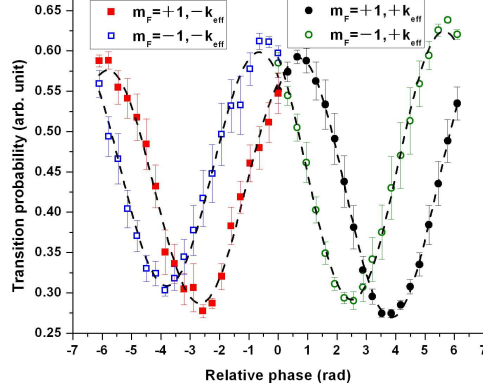


FIG. 2: (color online) Fringes for different combinations of  $m_F$  and  $k_{\text{eff}}$ , where each fringe shown is an average of 10 fringes with one corresponding combination. In one cycle, the fringes are obtained in turn for the combinations of  $m_F = +1$  and  $+k_{\text{eff}}$  (black circle),  $m_F = +1$  and  $-k_{\text{eff}}$  (red square),  $m_F = -1$  and  $+k_{\text{eff}}$  (olive empty circle),  $m_F = -1$  and  $-k_{\text{eff}}$  (blue empty square).

with a Raman  $\pi$  pulse applied at the right moment. Here the spectroscopies with the Raman lasers configured in  $+k_{\text{eff}}$  and  $-k_{\text{eff}}$  are combined to make a differential measurement, in which method the knowledge of the Zeeman shift or the AC-Stark shift is not needed. The measured average velocity is  $V_\pi = 509.0(1)$  mm/s for the selected atoms in  $|F = 1, m_F = +1\rangle$ , and is  $V_\pi = 509.4(1)$  mm/s for  $|F = 1, m_F = -1\rangle$  at the moment of the interfering  $\pi$  pulse.

Finally the measurement of the gravity acceleration of the atoms in different magnetic sublevels is performed sequentially, with different interfering configurations of the Raman lasers. One full interferometry fringe is obtained by scanning the chirp rate of  $\omega_{\text{eff}}$  in 20 steps for each  $m_F$  in each interfering  $k_{\text{eff}}$  configuration, namely 30 s for a full fringe. Meanwhile, in order to reduce the effect of possible drift of related quantities, for example, the Raman lasers power, four adjacent fringes are grouped as a cycle unit, with one fringe corresponding to one combination of  $m_F$  and  $k_{\text{eff}}$ . The switches between the combinations are automatically controlled by the computer through tuning the Raman lasers detune, and the typical fringes for the four combinations are shown in Fig.2. The measurement is repeated about 28 hours from cycle to cycle, and the phase shifts are extracted by the cosine fitting from the fringes. The differential mode result and the common mode result are obtained from the combinations of the corresponding phase shifts. The Allan deviation for the gravity acceleration measurement is calculated from the differential mode result for each  $m_F$ , which is shown in Fig.3, and the statistics of the combined measurement results for each  $m_F$  is

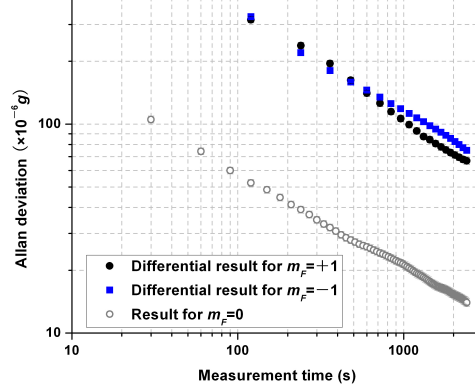


FIG. 3: (color online) Short-term Allan deviations for the gravity acceleration measurements using atoms in different  $m_F$ . The Allan deviations for  $m_F = +1$  (black circle) and  $m_F = -1$  (blue square) are calculated from the differential measurement results, while that for  $m_F = 0$  (gray empty circle) is calculated from the phase shifts obtained consecutively with Raman lasers always configured in  $+k_{\text{eff}}$ .

also acquired as shown in Table I. The Allan deviation for the measurement using the atoms in  $m_F = 0$  with the Raman lasers configured in  $+k_{\text{eff}}$  for  $T = 2$  ms is also shown in Fig.3 as a reference. According to the Allan deviations, the short term sensitivity for the interferometers using atoms in  $m_F = \pm 1$  is about  $3.4 \times 10^{-3} g / \sqrt{\text{Hz}}$ , which implies a sensitivity of  $2.4 \times 10^{-3} g / \sqrt{\text{Hz}}$  if only one combination of  $m_F$  and  $k_{\text{eff}}$  is consecutively repeated. This induced sensitivity is about four times worse than that using atoms in  $m_F = 0$ , which is most probably due to the fluctuation of the location where the atoms interacts with the interfering pulses (and thus the fluctuation of the experienced magnetic field gradient by the atoms). This fluctuation is caused by the variation of the launch velocity as well as the initial launch position of the atomic cloud from shot to shot.

The uncertainties in Table I are the corresponding statistical standard deviations. From the common mode results, the magnetic field gradients experienced for atoms in each  $m_F$  are deduced, which are nearly equal as expected since the interfering region is the same. According to Eq.(3), this gradient with a magnitude of  $-37 \mu\text{G}/\text{mm}$  corresponds to a  $+8$  mrad residual effect for the differential result with atoms in  $m_F = +1$ , and  $-8$  mrad residual effect for  $m_F = -1$ . It shows that a majority of the phase shift due to the magnetic field inhomogeneity is canceled in the differential measurement, and the residual is only about 1.2%. And the residual effect due to the Raman pulses durations is far less than that level, which is thus safely neglected in this work. In this differential measurement of the gravity acceleration with a rather short separation time, some disturbances,

for example, that induced by nearby masses or tilt of the Raman lasers, are common for the atoms in  $m_F = +1$  and  $m_F = -1$  and thus cancel in the final comparison, and other disturbances, for example, that induced by the AC-Stark shift or the Coriolis effect, can be neglected at the present level of accuracy. The Eötvös ratio is finally given by

$$\eta_S \equiv 2 \frac{g_+ - g_-}{g_+ + g_-} = 2 \frac{\varphi_{m_F=+1}^d - \varphi_{m_F=-1}^d}{\varphi_{m_F=+1}^d + \varphi_{m_F=-1}^d}, \quad (4)$$

where  $\Delta\varphi_{m_F}^d$  is the corrected differential results as listed in Table I. The resultant Eötvös ratio determined by this work is  $(-0.2 \pm 1.5) \times 10^{-5}$ , which indicates that the violation of WEP has not been observed at the level of  $1.5 \times 10^{-5}$  for the atoms with different polarization orientations.

In conclusion, we have tested UFF with atoms in different spin orientations based on a Mach-Zehnder-type atom interferometer, and the violation of UFF isn't observed at the level of  $1.5 \times 10^{-5}$ . This work represents the first atom interferometer which simultaneously measures the gravity acceleration and magnetic-field gradient, and also presents a direct test of spin-orientation related spin-gravity couplings on quantum basis. The present precision is limited by the fluctuation of the atomic fountain arising from the atom launch procedure. The influence of this fluctuation can be alleviated with a more homogeneous magnetic field in future measurement, and in this situation the pulses separation time can also be enlarged, which will effectively improve the interferometer sensitivity. On the other hand, the standing optical waves can be explored to manipulate the interfering of the atoms (see Ref. [27], for example), in which case the internal state of the atom doesn't change and thus the influence of the magnetic field inhomogeneity is dramatically decreased. We anticipate a better result for the UFF test with atoms in different spin orientations using interferometers of this kind in future.

TABLE I: Statistics of the differential mode measurement and the common mode measurement. The  $2\pi$  ambiguity is easily removed in this work thanks to the rather short separation time  $T$ . The magnetic field gradient is deduced from  $\Delta\varphi_{m_F}^c$ , and the corrected  $\Delta\varphi_{m_F}^d$  in the last column is the result of subtracting the residual magnetic field inhomogeneity effect from the original  $\Delta\varphi_{m_F}^d$  in the second column.

$m_F$	$\Delta\varphi_{m_F}^d$ rad	$\Delta\varphi_{m_F}^c$ rad	$\gamma_B$ $\mu\text{G}/\text{mm}$	Corrected $\Delta\varphi_{m_F}^d$ rad
+1	-644.322(7)	-0.674(8)	-37.6(4)	-644.330(7)
-1	-644.339(7)	+0.666(8)	-37.2(4)	-644.331(7)



We thank Zhifang Xu for enlightening discussions. This work is supported by the National Natural Science Foundation of China (Grants No. 41127002, No. 11204094, and No. 11205064) and the National Basic Research Program of China (Grant No. 2010CB832806).

---

\* E-mail: zkhu@mail.hust.edu.cn

- [1] C. Misner, K. Thorne, and J. Wheeler, *Gravitation* (Freeman, San Francisco, 1973).
- [2] Y. Su, B. R. Heckel, E. G. Adelberger, J. H. Gundlach, M. Harris, G. L. Smith, and H. E. Swanson, *Phys. Rev. D* 50, 3614 (1994).
- [3] J. H. Gundlach, G. L. Smith, E. G. Adleberger, B. R. Heckel, and H. E. Swanson, *Phys. Rev. Lett.* 78, 2523 (1997).
- [4] S. Schlamminger, K.-Y. Choi, T. A. Wagner, J. H. Gundlach, and E. G. Adelberger, *Phys. Rev. Lett.* 100, 041101 (2008).
- [5] T. M. Niebauer, M. P. McHugh, and J. E. Faller, *Phys. Rev. Lett.* 59, 609 (1987).
- [6] K. Kuroda and N. Mio, *Phys. Rev. Lett.* 62, 1941 (1989).
- [7] S. Carusotto, V. Cavasinni, A. Mordacci, F. Perrone, E. Polacco, E. Iacopini, and G. Stefanini, *Phys. Rev. Lett.* 69, 1722 (1992).
- [8] J. O. Dickey, P. L. Bender, J. E. Faller et al., *Science* 265, 482 (1994).
- [9] J. G. Williams, S. G. Turyshev, and D. H. Boggs, *Phys. Rev. Lett.* 93, 261101 (2004).
- [10] F. W. Hehl, P. von der Heyde, G. D. Kerlick, and J. M. Nester, *Rev. Mod. Phys.* 48, 393 (1976).
- [11] A. Peters, *Phys. Rev. D* 18, 2739 (1978).
- [12] B. Mashhoon, *Class. Quantum Grav.* 17, 2399 (2000).
- [13] Y. Z. Zhang, J. Luo, and Y. X. Nie, *Mod. Phys. Lett. A* 16, 789 (2001).
- [14] A. J. Silenko, O. V. Teryaev, *Phys. Rev. D* 76, 061101(R) (2007).
- [15] W. T. Ni, *Rep. Prog. Phys.* 73, 056901 (2010).
- [16] Z. K. Hu, Y. Ke, X. B. Deng, Z. B. Zhou, and J. Luo, *Chin. Phys. Lett.* 29, 080401 (2012).
- [17] H. Hayasaka and S. Takeuchi, *Phys. Rev. Lett.* 63, 2701 (1989).
- [18] J. E. Faller, W. J. Hollander, P. G. Nelson, and M. P. Mchugh, *Phys. Rev. Lett.* 64,825 (1990).
- [19] J. M. Nitschke and P. A. Wilmarth, *Phys. Rev. Lett.* 64, 2115 (1990).
- [20] D. J. Wineland, J. J. Bollinger, D. J. Heinzen, W. M. Itano, and M. G. Raizen, *Phys. Rev. Lett.* 67, 1735 (1991).

- [21] L. S. Hou and W. T. Ni, *Mod. Phys. Lett. A* 16, 763 (2001).
- [22] Z. B. Zhou, J. Luo, Q. Yan, Z. G. Wu, Y. Z. Zhang, and Y. X. Nie, *Phys. Rev. D* 66, 022002 (2002).
- [23] J. Luo, Y. X. Nie, Y. Z. Zhang, and Z. B. Zhou, *Phys. Rev. D* 65, 042005 (2002).
- [24] W. T. Ni, *Phys. Rev. Lett.* 107, 051103 (2011).
- [25] R. Colella, A. W. Overhauser, and S. A. Werner, *Phys. Rev. Lett.* 34, 1472 (1975).
- [26] A. Peters, K. Y. Chung, and S. Chu, *Nature (Lodon)* 400, 849 (1999).
- [27] S. Fray, C. A. Diez, T. W. Hänsch, and M. Weitz, *Phys. Rev. Lett.* 93, 240404 (2004).
- [28] S. Merlet, Q. Bodart, N. Malossi, A. Landragin, F. Pereira Dos Santos, O. Gitlein, and L. Timmen, *Metrologia* 47, L9-L11 (2010).
- [29] N. Poli, F.-Y. Wang, M. G. Tarallo, A. Alberti, M. Prevedelli, and G. M. Tino, *Phys. Rev. Lett* 106, 038501 (2011).
- [30] A. Bonnin, N. Zahzam, Y. Bidel, and A. Bresson, *Phys. Rev. A* 88, 043615 (2013).
- [31] D. Schlippert, J. Hartwig, H. Albers et al., *Phys. Rev. Lett.* 112, 203002 (2014).
- [32] C. Lämmerzahl, *Class. Quantum Grav.* 15, 13 (1998).
- [33] M. G. Tarallo, T. Mazzoni, N. Poli, D. V. Sutyurin, X. Zhang, and G. M. Tino, *Phys. Rev. Lett.* 113, 023005 (2014).
- [34] T. C. P. Chui and W. T. Ni, *Phys. Rev. Lett.* 71, 3247 (1993).
- [35] A. G. Glenday, C. E. Cramer, D. F. Phillips, and R. L. Walsworth, *Phys. Rev. Lett.* 101, 261801 (2008).
- [36] T. Lahaye, C. Menotti, L. Santos, M. Lewenstein, and T. Pfau, *Rep. Prog. Phys.* 72, 126401 (2009).
- [37] A. Peters, Ph.D. thesis, Stanford University, 1998.
- [38] Ch. J. Bordé, *Metrologia* 39, 435 (2002).
- [39] H. Müller, S. Chiow, S. Herrmann, and S. Chu, *Phys. Rev. Lett.* 100, 031101 (2008).
- [40] M. K. Zhou, Z. K. Hu, X. C. Duan, B. L. Sun, L. L. Chen, Q. Z. Zhang, and J. Luo, *Phys. Rev. A* 86, 043630 (2012).
- [41] Z. K. Hu, B. L. Sun, X. C. Duan, M. K. Zhou, L. L. Chen, S. Zhan, Q. Z. Zhang, and J. Luo, *Phys. Rev. A* 88, 043610 (2013).
- [42] R. Eötvös, V. Pekár, and E. Fekete, *Ann. Phys. (Leipzig)* 68, 11 (1922).
- [43] K. Moler, D. S. Weiss, M. Kasevich, and S. Chu, *Phys. Rev. A* 45, 342 (1992).
- [44] M. K. Zhou, Z. K. Hu, X. C. Duan, B. L. Sun, J. B. Zhao, and J. Luo, *Phys. Rev. A* 82, 061602(R) (2010).
- [45] Z. K. Hu, X. C. Duan, M. K. Zhou, B. L. Sun, J. B. Zhao, M. M. Huang, and J. Luo, *Phys. Rev. A* 84,

013620 (2011).

- [46] A. Louchet-Chauvet, T. Farah, Q. Bodart, A. Clairon, A. Landragin, S. Merlet, and F. P. Dos Santos, New J. Phys. 13, 065025 (2011).